Journal of Membrane Science 563 (2018) 54–64

Contents lists available at ScienceDirect

Journal of Membrane Science

journal homepage: www.elsevier.com/locate/memsci

Surface zwitterionization of PVDF VIPS membranes for oil and water separation

Antoine Venault[a,*], Chia-Yu Chang[a], Tai-Chun Tsai[a], Hsiang-Yu Chang[a], Denis Bouyer[b], Kueir-Rarn Lee[a], Yung Chang[a,*]

[a] Department of Chemical Engineering and R&D Center for Membrane Technology, Chung Yuan Christian University, 200 Chung Pei Rd, Taoyuan 320, Taiwan
[b] Institut Européen des Membranes, UMR 5635-CNRS, ENSCM, UM II, CC047, Place E. Bataillon, 34095 Montpellier, France

ARTICLE INFO

Keywords:
Combined polymerization/self-assembling
PVDF VIPS membrane
PS-*r*-PSBMA copolymer
O/W separation

ABSTRACT

This work aims at applying a combined polymerization and membrane surface-modification process, in order to hydrophilize poly(vinylidene fluoride) membranes prepared by vapor-induced phase separation (VIPS), and eventually make them suitable for low transmembrane pressure (ΔP = 0.5 bar) membrane separation of various oil-in-water (O/W) emulsions. Styrene and sulfobetaine monomers were mixed and allowed to react while the PVDF membrane was in contact with the reactive mixture, enabling self-assembling of the random polymer on the membrane as it was formed. Reaction parameters were optimized, and it was found that a solid content of 5 wt%, a styrene/SBMA ratio of 40/60 and a reaction time of 5 h led to very hydrophilic membrane (water contact angle: 12°). The combination of chemical analyses evidenced the successful and controlled surface modification process. Physical analyses showed that deviating from the optimized conditions of styrene/SBMA ratio led to the formation of agglomerates (styrene-rich or SBMA-rich), associated to low porosity, and high coating density. The membranes were used to separate emulsions of toluene/W, hexane/W, hexadecane/W, diesel/W and soybean oil/W, leading to separation efficiency of 99.0%, 99.2%, 99.1%, 99.0% and 99.0%, respectively. This work thus presents a new avenue for surface modification of membrane with extremely efficient copolymers for which there is no common solvent, and brings several evidences of the suitability of VIPS membrane for cost-effective membrane separation of various emulsions.

1. Introduction

A number of processes and technical solutions are available and have been proven to be adequate for efficient separation of oil and water from either water-in-oil (W/O) or oil-in-water (O/W) emulsions, such as gravity separation [1], air flotation [2] or centrifugation [3]. Over the past decade, membrane technology has emerged as an alternate O/W and W/O separation technique because it often leads to a faster and/or more cost-efficient separation, and it offers both reduced environmental impact and reduced footprint [4–10]. In addition to their potential efficiency for addressing the treatment of oil spills which are unwanted and uncontrolled, membranes for the separation of oil and water can be applied in particular in two major industries: petroleum industry and vegetable oil industry wherein oily and aqueous phases are likely to come into contact at different stages of the production [11,12].

In petroleum industry, water either enters refineries (raw water) or leaves it (wastewater), but both types of water have to undergo treatment stages. Raw water has to be screened for potential oil pollutant because serious scale, sludge or foaming may occur during the following processing stages, which is highly undesirable. Wastewater corresponds to all types of water generated during oil processing and do contain significant amount of free hydrocarbons which must be removed from the main stream. Thus, many different types of O/W effluents should be treated during oil production. Water-flooding technique shall also be mentioned here: the injection of water into the oil formation is likely to lead to the formation of two types of emulsions [13,14]. The first one is a W/O emulsion/mixture as the produced oil sent to separators and storage tanks is likely to contain residual water, while the second one is a W/O emulsion/mixture as recovered and re-injected water may contain residual oil.

In vegetable oil processing industry, wastewater high in organic compounds such as oil and fat residues is generated. In particular, chemical extraction processes involve the use of a solvent which is often hexane or a mixture of different hexanes [15], employed for its great ability to extract oil from seeds. Thus, hexane is likely to be found in

* Corresponding authors.
E-mail addresses: avenault@cycu.edu.tw (A. Venault), ychang@cycu.edu.tw (Y. Chang).

https://doi.org/10.1016/j.memsci.2018.05.049
Received 20 February 2018; Received in revised form 24 April 2018; Accepted 24 May 2018
Available online 26 May 2018
0376-7388/ © 2018 Elsevier B.V. All rights reserved.

wastewater of various process stages. Even though some recent works mentioned the development of membrane technology for the separation of oil and water from vegetable oil refinery [16,17] and despite a recent economical evaluation highlighting the advantage of introducing oil/water separation processes in wastewater treatment of food processing factory [18], O/W membrane separation has yet to be developed in the wastewater treatment facilities.

Very recently, several works have been published on the breaking of water and emulsions or the separation of similar mixtures, supporting the growing appeal of membrane technology for the separation of oil and water [19–37]. Most of these reports concern the breaking of O/W emulsions, for which the practical applications are more numerous. A review of recent works highlights that for O/W separation, the matrix is often a hydrophobic polymer membrane such as poly(tetrafluoroethylene), poly(vinylidene fluoride) or poly(ethersulfone) which has been hydrophilized. Popular techniques are the use of modified nanoparticles of TiO_2 or SiO_2 [21,23,24], or the incorporation of carbon nanotubes [30–33] to prepare composite membranes. The direct usage of more hydrophilic polymer such as chitosan or poly(acrylonitrile) is also mentioned [22,26] but this approach may lead to uncontrolled swelling of the membrane by the aqueous phase, which in turns affects the stability of the performances. Thus, hydrophobic materials are preferred for their mechanical properties.

Despite many tremendous efforts carried out by research institutes and membrane manufacturers over the past recent years, a number of challenges still need to be overcome and many questions remain unanswered. They concern (i) the membrane preparation process, (ii) the membrane hydrophilization and (iii) the specificity of the emulsion. Starting with the membrane preparation process, in order to achieve energy-efficient (gravity-driven or low transmembrane pressure separation) and fast separation, the ideal membrane for O/W or W/O separation must be highly porous (open pores, UF/MF domain, porosity larger than 70%). There is a growing tendency to design electrospun membranes to match these structural requirements [28,32,34,36,37]. High separation rates are reported, but this process involves long spinning times (several hours), and some recent designs often include surface functionalization in one or several steps, which questions the feasibility of mass-production. Contrariwise, no study reports the use of the VIPS process, yet a controllable process involving significantly shorter membrane formation steps (typically less than 20 min), still leading to highly porous membranes. Secondly, even though they are the object of extensive studies on the design of nonfouling membranes [38–41], there is still no easy way to modify a highly porous hydrophobic membrane using a zwitterionic polymer. Zwitterionic materials are ideal candidate for surface hydrophilization, and so, could be promising surface-modifiers for O/W separation membranes. Surely, many grafting techniques exist but they often involve the use of surface-modification processes such as plasma-treatment or UV-treatment which are expensive and difficult to control at larger scale [38,40]. This is much harder to use a simpler coating procedure, because solubility issue arises when combining the zwitterionic moieties with more hydrophobic chains that would interact with the membrane system: it is extremely challenging to find non-aqueous solvents for zwitterionic copolymers as the zwitterionic head is usually highly hydrophilic while the anchoring units are highly hydrophobic. As a consequence of the lack of ideal solvent for zwitterionic sulfobetaine methacrylate (SBMA)-based copolymers, surface zwitterionization by dip-coating or thermal evaporation coating are not reported. To overcome this problem, Zhou *et al.* presented a work in which they first synthesized poly(sulfobetaine methacylate) PSBMA, followed by the co-deposition of PSBMA with dopamine solubilized in tris-buffer [42]. The use of polydopamine aimed at assisting the deposition of PSBMA at the surface of the membrane, without the formation of any covalent bonds between polydopamine and PSBMA. This coating procedure remains to this day a very unique work, to our knowledge, presenting a one-step coating of PSBMA but stability could be questioned. Finally, another challenge concerns the versatility of the separation. Outstanding results have been published in terms of separation efficiency, usually reaching 99% or higher. But in most cases, researchers focus on one or two types of emulsions, and once the concept proven, do not challenge their system against multiple and various O/W systems. These three identified challenges clearly highlight the need for more research works and extensive studies in this direction.

Based on these observations, we prepared poly(vinylidene fluoride) (PVDF) membranes by vapor-induced phase separation (VIPS) process, which, through a fine tuning of process parameters, leads to highly porous symmetric matrices with open large pores and high surface porosity, unlike the more common liquid-induced phase separation process which, using water as the non-solvent, leads to asymmetric finger-like structures, with both smaller surface pore-sizes and surface porosity, inadequate for the intended application. Then, we applied a surface-modification process which consists in polymerizing a random polymer – made here of polystyrene and poly(sulfobetaine methacrylate) – and coating the membrane in one single step. This combined synthesis and surface-modification process not only permits to save time but more importantly, it should address the solubility issues above-mentioned. It has to be optimized though, which constitutes the first part of the present report. After characterizing the physicochemical properties of the membranes and their wettability in a second part, we applied our membranes in the separation of various O/W emulsions, using low transmembrane pressure ($\Delta P = 0.5$ atm) membrane filtration. In particular, we tested toluene/W, hexane/W, hexadecane/W, diesel/W and soybean/W, in order to discuss, from the filtration rates and separation efficiencies obtained, the versatility of these modified VIPS membranes.

2. Materials and methods

2.1. Materials

PVDF material was purchased from Kynar®. It has an approximate molecular weight of 150,000 g/mol. It was washed repeatedly with ethanol and water in order to remove the impurities. The organic solvent used to prepare casting solutions was N-methylpyrrolidone (NMP), bought from Tedia. It was used directly as is. Styrene (Mw: 104.15 g mol^{-1}) and SBMA (Mw: 104.15 g mol^{-1}) monomers were both purchased from Sigma Aldrich. 2,2′-Azobis(2-methylpropionitrile) (AIBN) was purchased from Alfa Aesar. Methanol, solvent for the polymerization reaction, was bought form Sigma Aldrich. DI water (with a minimum resistivity of 18 Ω cm) was obtained from a Millipore purification system. Toluene was obtained from ECHO chemical Co and used without further purification treatment. Hexane, heptane and hexadecane were purchased from Uni-Onward Corp (Taiwan). Diesel oil was obtained from CPC Corporation, Taiwan. Vegetable soybean oil was purchased from Uni-President. The mixture of sulfur dioxide, iodine and imidazole (titrant), methanol (solvent) and imidazole (the organic base) used in Karl-Fisher test were obtained from Fluka and used directly without any pre-treatment step.

2.2. Methods

2.2.1. Preparation of casting solutions

The casting solutions were prepared by mixing 20 wt% of PVDF and 80 wt% of NMP. The temperature of dissolution was set to 32–35 °C. This parameter is essential to control the final morphology of the membranes [43,44]. Briefly, if the temperature is high (higher than the critical gelling dissolution temperature of about 32 °C), the nuclei density in the solution available for growth by crystallization will be low. Thus, the nuclei will have the possibility to grow, then leading to nodular membranes which are quite weak. On the other hand, a low dissolution temperature ensures a high nuclei density and during membrane formation, these nuclei cannot grow. As a consequence, the

structure of membranes is close to be a bi-continuous structure, much more strong. At the temperature chosen, it took about 9 days to obtain homogeneous solutions. Once ready, they were degassed for a few hours, and immediately used for membrane casting.

2.2.2. Preparation of PVDF membranes

Casting solution, glass plate onto which the casting solutions were cast, and metal casting knife were placed inside a VIPS process chamber. The relative humidity and the temperature were set to 70% and 30 °C, at least one hour before casting the solution. The relative humidity and the temperature, computer-controlled, were monitored by several sensors positioned at different locations in the chamber. Once the equilibrium in the chamber was reached, polymeric solutions were cast on a glass slide. Their initial thickness was 300 µm. Then, water vapors were allowed to penetrate in the polymeric system for 20 min. Thereafter, the films were immersed in DI water for 24 h to remove all traces of solvent. The water bath was changed once during this process. Finally, membranes were dried in normal conditions of temperature and pressure, and stored at 4 °C.

2.2.3. Surface modification of PVDF membranes

Membranes were modified by a self-assembling process which was conducted in the same time as the polymerization of the surface-modifier. To do so, styrene and sulfobetaine methacrylate monomers were mixed in a flask, together with AIBN (such as the total styrene/SBMA monomer to AIBN molar ratio was 125:1) and methanol, the solvent of the reaction. The membrane surface to be modified was positioned in such a way that it was in contact with the reactive mixture all along the polymerization process, as schematized in Fig. S1. Doing this, we aimed at anchoring the random polymer as it was formed through the polymerization reaction. The temperature of the reactive mixture was set to 60 °C. Parameters to adjust in order to optimize the membrane hydrophilic properties were the reaction time (0–24 h), the monomer solid content (0–10 wt%) and the styrene/SBMA monomer ratio (100/0–0/100). Their effect will be further discussed in subsequent sections. It was verified in preliminary tests that the positioning of the substrates in the reaction solution has little effect on the mass amount loaded on the membranes. In other words, in similar conditions of modification (similar molar composition, reaction time and solid content), it did not affect neither the surface porosity nor the coating density of the matrices, and the FT-IR patterns of the membrane surfaces were similar (Fig. S2). Once the reaction time reached, the flask containing the mixture and the membrane was immersed in an ice bath, to stop the polymerization. The membranes were then washed with DI water to remove the loosely adhering random polymers from the surface. Then, the samples were dried, and stored at 4 °C until use. One has to be reminded at this point that there is no common solvent for the copolymers of styrene and SBMA, which led us to use the combined synthesis/surface-modification process permitting to still take advantage of the anchoring ability of styrene and of the antifouling property of SBMA during the formation of the copolymers. The absence of solvent for the copolymer also implies that no direct information related to the characterization of the copolymer anchored to the membranes, in particular the molecular weight, is obtainable. This may be viewed as a drawback of this combined process.

2.2.4. Physico-chemical characterization of membranes

The surface chemistry of membranes was characterized by ATR-FT-IR, mapping FT-IR and XPS. For FT-IR measurements, a Perkin-Elmer Spectrum One instrument was employed. The internal reflection element was a ZnSe crystal. Each spectrum was captured by averaging 32 scans, at a resolution of 4 cm^{-1}. Mapping FT-IR was performed with a system combining a Jasco 6700 FT/IR instrument, a Jasco IRT-5200 microscope, a Jasco IPS-5000 automatic stage and a MCT-MD detector. Before image acquisition, the samples were freeze dried, and then fixed on a glass slide side by side. Mapping was conducted in reflection mode with a x16 Cassegrain objective lens. Each point was scanned 32 times at a 4 cm^{-1} resolution. The resulting images were color-coded from dark blue (no functional group at the wavenumber of interest) to red (high density of functional group at the wavenumber of interest). For XPS measurements, we used the same instrument and followed the same experimental procedure as earlier described [45]. Scanning electron microscope (SEM) images were obtained from a Hitachi S-3000 instrument. Prior to observation, the samples were mounted on SEM holders using double-sided adhesive tape, and sputter with gold for 2.5 min. Once the holder positioned in the SEM chamber, the accelerating voltage of the SEM was set to 3 keV, and observations carried out. 3 images of the membranes' surface are presented for each condition of surface modification in the Supporting Information section (Fig. S3).

The pore size of the virgin PVDF membrane was determined using a capillary flow porometer (CFP-1500-AXEL, PMI). The procedure used for this measurements is described elsewhere [46]. The porosity was assessed by immersing membrane samples (membrane diameter 1.3 cm) in ethanol. From the knowledge of the dry weight of the membranes, their wet weight, along with the density of PVDF (ρ_{PVDF} = 1.78 g/cm^3 at 25 °C) and that of the alcohol ($\rho_{Ethanol}$ = 0.79 g/cm^3 at 25 °C), the porosity could be evaluated according to the method and formula reported in Gu and coworker's study [47]. As a first assumption, we considered that the random copolymer did not significantly affect the density of the polymeric system.

The hydrophilicity in air and oleophilicity under water were evaluated by contact angle measurements. For water contact angle (WCA) measurements, membranes were stuck on a microscope glass slide using double-sided adhesive tape. The glass slide was positioned onto the stage of an automatic contact angle meter (OCA15EC, Dataphysics). 4-µL DI water droplets were dropped onto the membrane. After 5 s, a picture of the droplet deposited onto the surface was taken with a MDK 15EC camera (equipped with a ATL 2 × lens), and the water contact angle was automatically measured with the SCA20 software associated to the instrument. 10 independent measurements were performed for each condition of surface modification, and the averages obtained were taken as the WCA of the samples. For oil contact angle, membrane were also fixed to a glass slide, which was turned up-side down. The edges of the slide were put on a small DI-water container, and the surface of the membrane was immersed in the DI-water bath (the procedure is presented in Fig. S4). Then, oil droplet was injected in the water bath underneath the membrane surface. The oil droplet travelled toward the membrane surface, due to gravity difference. Once in contact with the membrane, a picture was shot and the OCA determined similarly as the WCA. This procedure was repeated 5 times for each conditions of surface modification (so, for each type of membrane) and for each oil used in the filtration tests.

2.2.5. Separation of O/W emulsions

Emulsions were prepared by mixing oil (toluene, hexane, hexadecane, diesel, soybean oil) and water, such that the oil/water ratio was 1:99 [48]. A total volume of 50 mL was prepared. The mixture was sonicated using an ultrasonic bath (DC200H), operating at a frequency of 40 kHz, and a 200 W output power for 1 h. The emulsions size was assessed by DLS at 25 °C, using a DeltaTM NanoS Particle Analyzer instrument (Beckman Coulter®). The emulsion to analyze was disposed in a Y-shape micro-cuvette. DLS also permitted to verify that the emulsions were stable for a period of time longer than the duration of the filtration tests. Microscope observations of the different emulsions (feed for filtration) and permeates were taken using a Nikon DS-Ri 1 microscope. The selected membrane (filtration area: 3.14 cm^2) was placed in a filtration cell connected to a 250-mL reservoir. The reservoir was connected to a nitrogen tank. An overpressure (1 atm) DI-water cycle was run until reaching steady state water flux. Then, DI water was replaced by the emulsion and the pressure decreased to 0.5 atm. The change in permeate weight was continuously recorded with a METTLER

TOLEDO balance positioned underneath the cell (which thus enabled to monitor the flux), linked to a laptop equipped with SerialPortToKeyboard software. Once the permeate weight reached a plateau, indicating the end of the filtration, the tests were stopped and we proceeded to the analysis of the different phases.

The composition of the phases after filtration was determined using a Karl-Fisher instrument, enabling to measure the water content in the sample tested. In this test, the end of the titration is sensed by a dual platinum pin electrode (model DM 143-SC, METTLER TOLEDO). From the knowledge of the water content in the permeate and in the feed, one can readily evaluate the separation efficiency of the membrane.

3. Results and discussion

3.1. Optimization of the self-assembling process

At first, some efforts were needed to optimize the surface modification process of the membranes, because we have very little knowledge on this combined polymerization of styrene (ST) and sulfobetaine methacrylate (SBMA) units and self-assembling process. Some of the main parameters identified as potentially influencing the final surface modification were the reaction time, the ST/SBMA ratio and the total solid content in the mixture. We proceeded by trial and error, and started by fixing the reaction time to 24 h and the solid content to 5 wt %. Then, we looked into the influence of the ST/SBMA on the surface hydrophilization of the membranes, which was assessed by measuring the water contact angle in air of the membranes at t = 5 s. The related results are presented in Fig. 1a. Two main regions can be highlighted. For ST/SBMA equal to/lower than 0.5, the WCA was found to be lower than 55°, which represents a major improvement, as the WCA of the pristine membrane was 118 ± 5°. On the other hand, for a ST/SBMA ratio higher than 0.5, WCA ranged between 86 ± 4° and 114 ± 4°. Several comments can be made at this stage. First, despite the total absence of anchoring unit in the structure, it appears that there can still be entrapment of SBMA units within the porous domains of the VIPS membrane, since ST0SB100 membrane exhibit a WCA of 48 ± 5°. It suggests that PSBMA grew and formed polymer aggregates that precipitated in the solution or inside the pores of the membrane. Knowing that PSBMA polymer is extremely hydrophilic while PVDF is hydrophobic, there cannot be any chain interactions that would stabilize the system formed such that at some point, it is expected that PSBMA will be released off of the membrane. Stability can only be provided by styrene groups, forming hydrophobic-hydrophobic interactions with PVDF as proven earlier by Chiag *et al.* [49] and Lin *et al.* [50] after coating PVDF membranes with a copolymer of styrene and poly(ethylene glycol methacrylate). Thus, a slight increase of styrene amount (from ST10SB90 to ST40SB60) enables to decrease the WCA because the surface modification is more stable, such that more polymer chains can interact with PVDF than in the case of ST0SB100. Increasing the ST/SBMA ratio a little more should permit to enhance the interactions between the random copolymer and the polymer matrix, but it is also associated with a decrease of hydrophilic units in the polymeric surface-

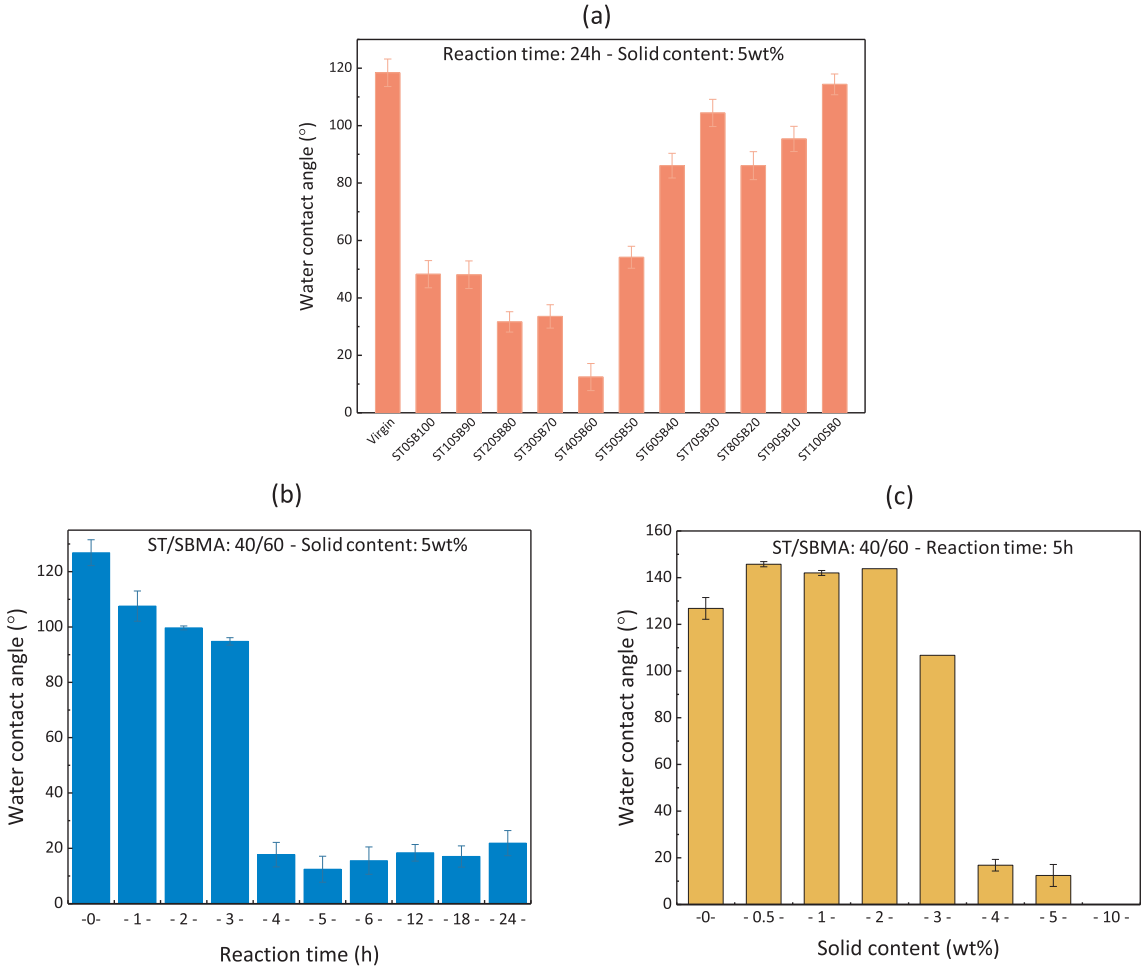

Fig. 1. Optimization of the surface-modification process by measuring the water contact angle after 5 s (a) Effect of the ST/SBMA monomer ratio on the surface hydrophilization of PVDF membrane. *Reaction time: 24 h, Solid content 5 wt%* (b) Effect of the reaction time on the surface hydrophilization of PVDF membrane. *ST/SBMA: 40/60, Solid content 5 wt%* (c) Effect of the solid content on the surface hydrophilization of PVDF membrane. *ST/SBMA: 40/60, Reaction time: 5 h.*

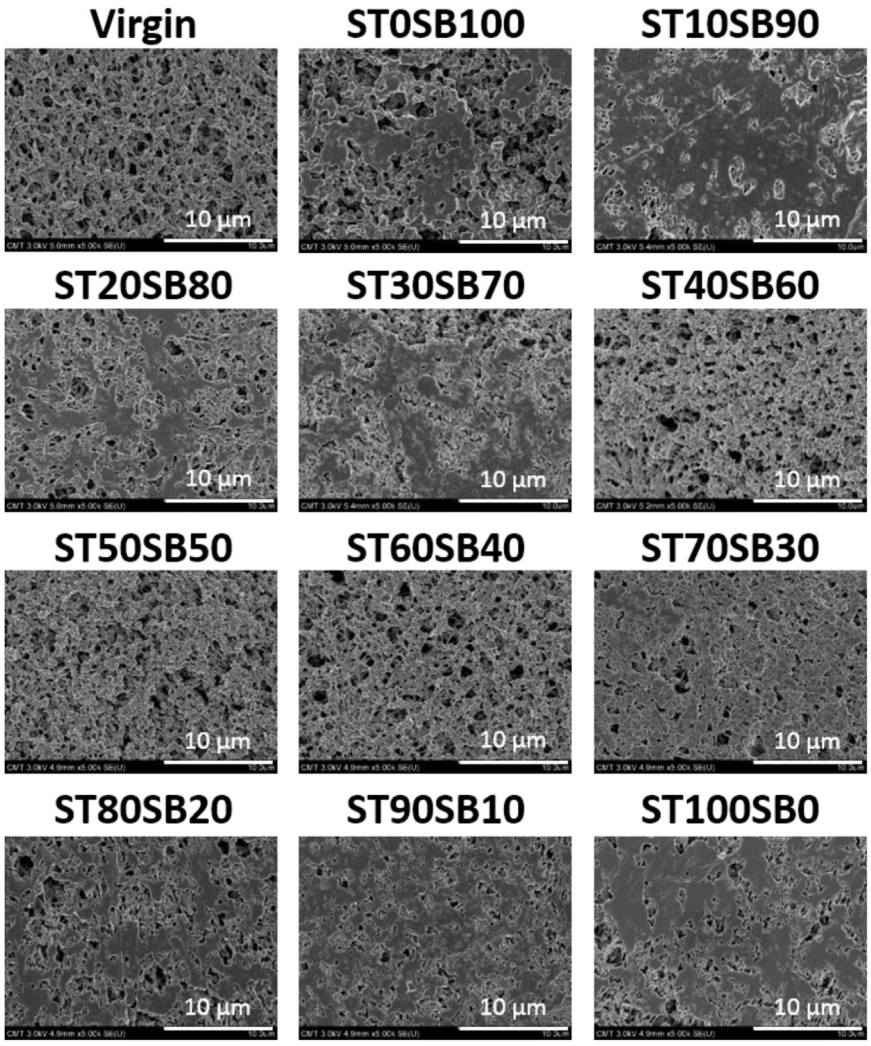

Fig. 2. SEM images of the virgin and surface-modified membranes.

modifying layer. Therefore, the WCA cannot be further lowered, as seen for membranes from ST60SB40 (WCA of 86 ± 4°) to ST100SB0 (WCA of 114 ± 4°). Finally, our results tend to indicate that a ST/SBMA ratio of 40/60 leads to the lowest WCA: 12 ± 5°. For this ratio only, results suggest that there is an ideal compromise between the amount of styrene anchoring units, and the amount of hydrophilic moieties (SBMA) that enables anchoring of the copolymer and the formation of a tight hydration layer around the SBMA moieties, eventually leading to the best surface wettability by water. Thus, this ratio was fixed in the following optimization tests.

In a second step, we analyzed the effect of the reaction time on the WCA of the different membranes (fixing the ST/SBMA ratio to 40/60 for all membranes). The solid content was still fixed to 5 wt%, and reaction time ranged between 1 h and 24 h. Related results are presented in Fig. 1b. This figure unveils that the WCA keeps on decreasing from 1 to 5 h, with WCA found to be 108 ± 5°, 100 ± 1°, 95 ± 1°, 89 ± 1° and 12 ± 5° for reaction time of 1, 2, 3, 4 and 5 h respectively. However, as the exposition of the membrane to the reactive mixture was further extended, no more decrease of the WCA could be measured. This observation may be associated to several phenomena. First, the membrane may be saturated with random copolymer after 5 h. Second, as the time is extended, the polymerization keeps going such that the random polymer chains grow. It is likely that the chains have reached a size/configuration preventing the self-assembling process to occur and leading to their precipitation in the solution instead. Thirdly, the polymer formed is a random copolymer. This implies that all hydrophobic chains are not necessarily favorably oriented toward the matrix to form hydrophobic interactions with PVDF, but instead are oriented toward the bulk of the solution. So, when longer reaction times are at play, the randomness of the polymer can lead to copolymer interchain interactions, rather than copolymer-matrix interactions only. This leads to surface heterogeneity, which can also contribute to an increase of WCA. In the same time, longer hydrophilic chains are obtained arising from the longer reaction times, and leading to lower WCA. Eventually, both effects tend to annihilate, hence the plateau reached for WCA. Eventually, 5 h appeared to be the optimum time.

The third test consisted in selecting the most appropriate solid content. The range chosen was 0.5 wt% − 10 wt%. Again, the lowest WCA after 5 s was the selection criterion. Fig. 1c shows that for contents lower than 4 wt%, surface modification is not efficient or at least, does not permit to obtain a fast wetting of the membranes as the water contact angle after 5 s remained as high as that of the virgin membrane. However, from a 4 wt%, a drastic improvement was observed, as the WCA at the same time was as low as 17 ± 3°. For 10 wt%, membrane wetting was immediate with a zero WCA instantaneously measured. It was decided to keep the solid content to 5 wt%: using twice as much reactants (10 wt%) is not justified by the slight wetting improvement, but costs much more, and more importantly, leads to quite weak membranes difficult to handle.

In conclusion of this section, the following parameters were chosen to conduct the O/W emulsion separation: ST/SBMA ratio: 40/60; reaction time: 5 h and solid content: 5 wt%. In the next section focusing

on the physicochemical characterization of the membranes, the solid content and reaction time are fixed to the determined value, but we still use varying ST/SBMA ratio to get further insights into the impact of this essential parameter on membrane structure and surface chemistry, and also to try to improve our understanding of the results of Fig. 1a, in particular those revealing that despite low styrene content, the WCA of the modified membrane (e.g. ST10SB90, ST0SB100) was still low, which would suggest that SBMA was still deposited.

3.2. Physicochemical characterization of membranes

A number of characterization methods was used to analyze the surface physicochemical properties of the membranes. Starting with the surface structure, SEM observations were conducted and the related images are presented in Fig. 2 and Fig. S3. For each surface, three images are presented in Fig. S3 taken at random position onto the membrane. The virgin PVDF membrane exhibits a classic structure having a mean pore flow diameter found to be 0.088 ± 0.012 µm, close to be bi-continuous with very small nodules forming the polymer-rich domains, because the temperature of dissolution of the dope was close to the critical gelling temperature [43,44]. Exposing the membrane surface to the polymerization bath led to significant changes, regardless of the actual composition of the reactive mixture.

First it is seen that at low styrene content, aggregates were formed at the surface of the membranes. This is particularly striking for ST0SB100 to ST30SB70 membranes, and this confirms that despite low anchoring block content in the solution, hydrophilic moieties could be trapped between the porous domains of the pristine membrane and grow, then contributing to a significant decreasing of the surface porosity compared with that of the virgin membrane (71 ± 2%). Indeed, the results of Fig. 3 show that the porosity of ST0SB100 was as low as 50%. Aggregates are formed of a majority of hydrophilic moieties. Because only low energy interactions are at play (no covalent bond between PVDF and the copolymer), they are not expected to interact and to self-organize in a controlled fashion with PVDF. Lack of stability can be expected and is proven in Fig. S5 (Supporting information) showing that after 1 week-immersion in DI water, the agglomerates of PSBMA vanished from the surface of the PVDF membrane. The rationale for the formation of these aggregates despite low concentration of styrene is as follows: during continuous stirring of the solution, the newly formed hydrophilic polymer molecules will randomly make contact with the membrane and differences of polarity will make the SBMA-rich molecules form heaps weakly anchored to the membrane and trapped in the pores.

But it cannot be denied from these images that pure SBMA polymer can interact with PVDF membrane despite the absence of hydrophobic-

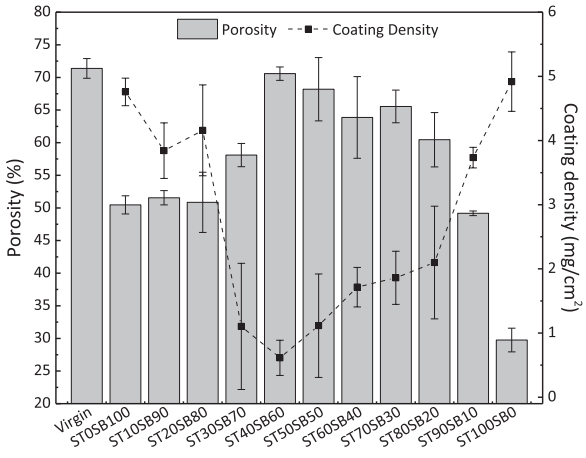

Fig. 3. Effect of ST/SBMA monomer ratio on the surface porosity and coating density of membranes.

hydrophobic interactions, and this observation can also be correlated to the results of Fig. 1a that showed a significant decreasing of WCA for ST0SB100. The SEM images of membranes incubated in the bath containing a majority of styrene monomers (from ST70SB30 to ST100SB0) also revealed the appearance of dense domains heterogeneously distributed. These domains are formed of copolymer containing a majority of anchoring units in the backbone. Consequently, they should be more stable than those involved in the modification of ST0SB100 to ST30SB70 membranes, which was proven by the results of Fig. S5 showing that agglomerates of polystyrene are still visible after 1-week-immersion in DI-water. Yet the results also revealed that in these formulation conditions (large excess of styrene), the surface modification could not be homogeneously achieved. Freitas Siquiera *et al.* reminded that the interfacial tension between PVDF and polystyrene was high [51], which probably has driven local segregation of polystyrene domains and the formation of polystyrene aggregates. However, the porosity of these membranes remained in the same order of magnitude as that of the virgin PVDF membrane, suggesting that the aggregates formed were smaller than in the case of SBMA aggregates. The third group of membrane is composed of ST40SB60, ST50SB50 and ST60SB40 membranes. These membranes seem much more homogeneous, as far as their surface is concerned, which suggests that for a ST/SBMA ratio close to 50%, the surface modification process is better controlled. For these ratios, the random polymers formed preferentially interact with the PVDF matrix through their PS units, rather than forming intermolecular interactions as in the case of SBMA or styrene excess. We admit that more evidence on the composition dependence of the reaction bath on the nature of the interactions established during the reaction/deposition process, i.e. self-interactions or interactions with the substrate, is needed. Nevertheless, the analysis of the surface of the membrane do show that the molar composition of the reaction/deposition bath is a key parameter to take into account to reach homogeneous membrane surfaces.

Also, although copolymers of styrene and SBMA have never been employed in coating, to the best of our knowledge, because of the absence of common solvent for the copolymers, one can still qualitatively assess the suitability of the one step polymerization/modification process by referring to observations reported in literature. As earlier described for copolymers used to coat PVDF membranes also containing styrene as the anchoring block (as in the present work), but poly (ethylene glycol methacrylate) as the antifouling moieties, an unchanged surface morphology after the modification process, compared to the virgin membrane, is a first indication of homogeneous modification, which also signifies the suitability of the modification process [50]. Therefore, the SEM images of Fig. 2 corresponding to the membranes obtained in the particular conditions of ST/SBMA ratio close to 50% suggest regular anchoring of the copolymers and the absence of aggregates. This is further supported by the evaluation of the coating density. It is seen on Fig. 3 that as the styrene/SBMA ratio deviates from 1, the coating density dramatically increases to reach uncommon values, up to 5 mg/cm^2 for ST0SB100, which clearly suggests that aggregates were formed at the surface of the membranes when an excess of either SBMA or styrene was employed in the reaction bath. On the other hand, in the optimized conditions of reaction bath composition, much lower coating densities were measured, comparable to those obtained after homogeneous coating of copolymers of styrene and PEGMA on UF PVDF membranes [49].

The surface chemistry of the membranes was analyzed by FT-IR and XPS. Here, we selected the virgin membrane, SB100ST0, ST100SB0 and the optimized membrane ST40SB60. Starting with the FT-IR measurements displayed in Fig. 4, they tend to confirm that self-assembling of the random copolymer (or polymer in the case of ST100SB0 and ST0SB100) occurred regardless of the composition of the reaction mixture. Except for ST100SB0, a peak can be seen at 1730 cm^{-1}, attributed to the stretching of the C=O function of SBMA moieties [52]. Its intensity logically increases as the ST/SBMA ratio decreases, and is still

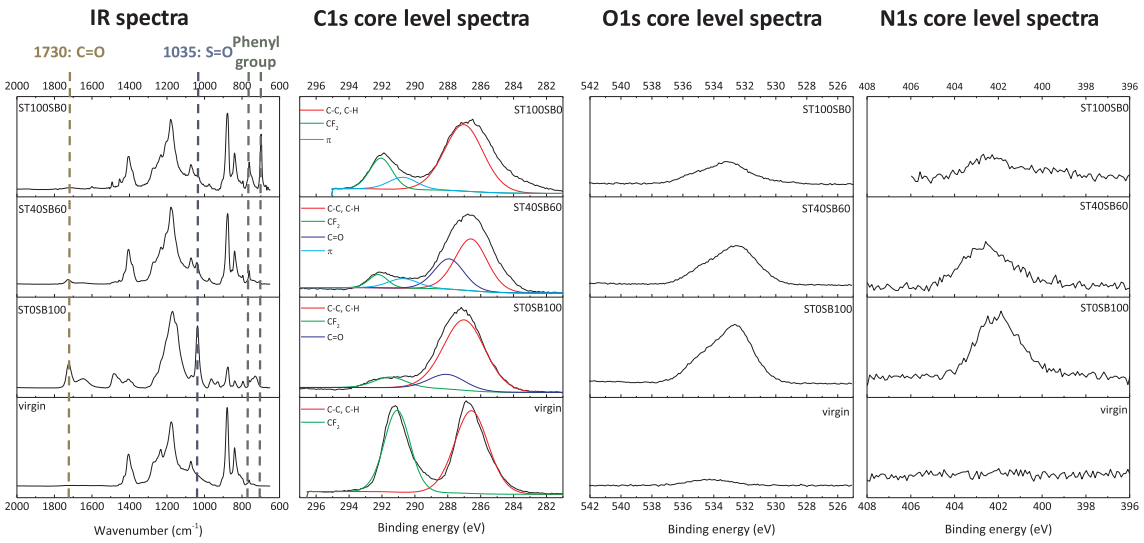

Fig. 4. Chemical characterization of virgin, ST0SB100, ST40SB60 and ST100SB0 membranes.

visible after several weeks immersion in methanol, indicating a quite stable anchoring of the copolymer on the surface of the membranes (Fig. S6). The spectrum of ST0SB100 is significantly different from that of virgin and other membranes, due to the deposition of numerous SBMA aggregates at the surface of the membranes, as evidenced and discussed earlier. In particular, the intensity of the peaks due to the carboxylate (stretching of -C=O) and the sulfonate (symmetric stretching of S=O in $-SO_3^-$) functions found at 1730 cm^{-1} and 1035 cm^{-1}, respectively, are significantly higher than in any other spectra [53]. The spectrum of ST100SB0 is also very original as compared to the others, because only polystyrene was deposited onto the membranes. The two high intensity bands observed at 760 cm^{-1} and 700 cm^{-1}, and attributed to the stretching of the sp^2 structure [54], clearly indicate that polystyrene interacts with the PVDF matrix. The intensity of these bands decreases as the ST/SBMA ratio decreases. For ST40SB60, the characteristic bands of both the anchoring block (PS) and the antifouling block (SBMA) are well detected at 760 cm^{-1} and 1730 cm^{-1}, respectively, which indicates that the surface modification of the membrane is effective.

Further information can be obtained by analyzing the XPS spectra presented on this same figure. In particular, we reported the detailed C1s, O1s and N1s core-level spectra of the membranes. It is first seen from the N1s and O1s spectra that except for the virgin and the ST100SB0 membranes, the presence of nitrogen and oxygen can be detected, attributed to the zwitterionic moieties. It is also worth noting that these spectra confirm the presence of SBMA moieties at the surface of the membrane even if there is no anchoring (styrene) group (ST/SBMA = 0), which totally correlates with the conclusion drawn from the SEM pictures: SBMA can be temporarily deposited onto PVDF membranes, even without styrene monomer in the reactive mixture, and forms aggregates. The chemical functional groups were also identified on the C1s core level spectra presented in Fig. 4. In particular, the peak observed at a binding energy BE = 288 eV is attributed to the [O-C=O] group in SBMA [55]. It was also seen that the characteristic signal of carbon-fluorine bond at BE = 292.6 eV tends to disappear after surface-modification, which proves that interactions are established between PVDF and the surface-modifier, regardless of its nature. XPS characterization was also useful to evaluate the actual ST/SBMA ratio and so the composition of the random polymers coated at the surface of the membranes. We used the C1s core level spectra, and more particularly the signal of the aromatic functional groups of styrene (BE_{π} = 290.8 eV) [56] and that of the ether functional groups of SBMA ($BE_{O\text{-}C\text{=}O}$ = 288.0 eV). The ratio of these signals' intensity was calculated and results are presented in Table 1. The calculated ratios are close to the initial molar ratios in the reactive solution (theoretical ratios), suggesting similar reactivity of the monomers during the growth and deposition of the copolymers. Finally, the O1s and N1s core-level spectra also confirm the effective surface modification of the different membranes. A large peak at BE = 532.6 eV is seen on the O1s spectrum of ST0SB100 and ST40SB60 membranes, attributed to the [O-C=O] group in SBMA. A slight peak is also seen on the spectrum of ST100SB0 membrane, which might be due to residual products of styrene oxidation. Finally, a high-intensity peak is seen on the N1s spectrum of ST0SB100, at a BE of 402.2 eV, attributed to quaternary amine functional group of SBMA, thus confirming again the deposition of SBMA on the sample. Logically, this peak is also detected on ST40SB60 membrane, but at a lower intensity.

Table 1
Theoretical vs. actual styrene/SBMA composition at the surface of membranes.

Membrane ID	Styrene/SBMA ratio in the reactive bath	Styrene/SBMA ratio calculated from XPS characterization
ST0SB100	0:100	0:100
ST10SB90	10:90	13:87
ST20SB80	20:80	15:85
ST30SB70	30:70	20:80
ST40SB60	40:60	39:61
ST50SB50	50:50	54:46
ST60SB40	60:40	57:43
ST70SB30	70:30	70:30
ST80SB20	80:20	76:24
ST90SB10	90:10	87:13
ST100SB0	100:0	100:0

Finally, a comparative ATR-FTIR mapping analysis of the virgin and ST40SB60 membranes was carried out at 1730 cm^{-1} (C=O functional group of SBMA) to assess the distribution of the random polymer at the surface of the membrane. If dark blue regions are the areas where no copolymer is grafted and logically entirely cover the map of the virgin membrane, the color-coded results presented in Fig. 5 highlight that the map of ST40SB60 is dominated by green and orange colors, with very little blue spots, hence indicating the presence of copolymer over the entire scanned area. In conclusion, ATR-FTIR mapping also proves that PS-*r*-PSBMA is quite homogeneously distributed at the surface of ST40SB60 membrane.

The wettability of the membranes by different oils under water was also investigated (Fig. 6). It is first seen that the virgin membrane is rather oleophilic, with OCA measured to be 51 ± 9°, 56 ± 5°, 54 ± 5° and 73 ± 10° using toluene, hexane, diesel and soybean oil,

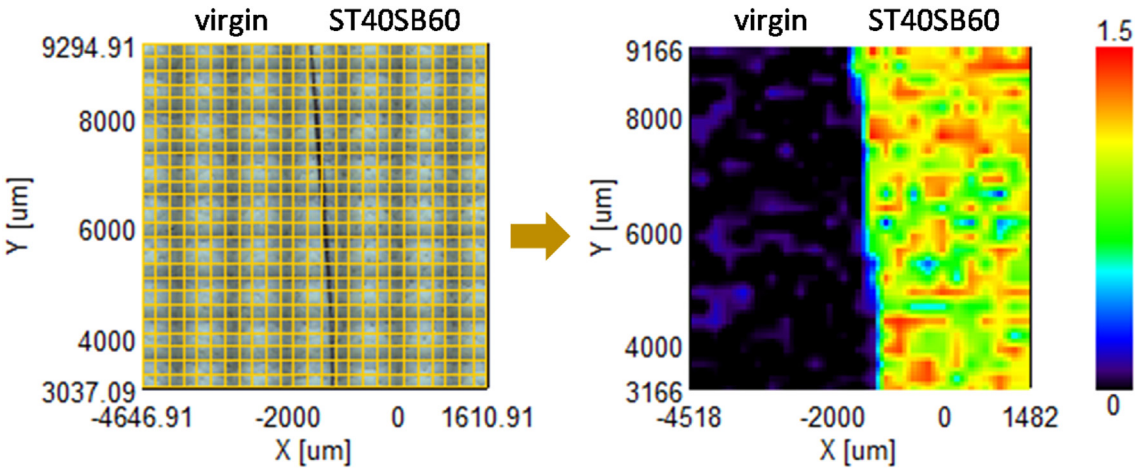

Fig. 5. ATR-FTIR mapping analysis of the virgin and ST40SB60 membranes at 1730 cm^{-1}. The left panel presents the microscope image corresponding to the scanned areas while the right panel presents the color-coded images.

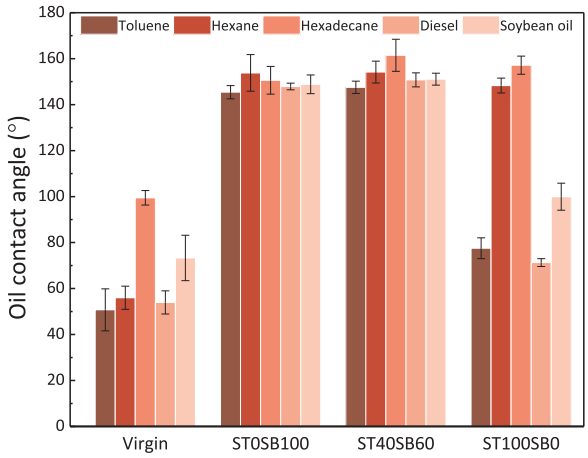

Fig. 6. Oil contact angle under water of the virgin, ST0SB100, ST40SB60 and ST100SB0 membranes after 5 s contact between the droplet and the membrane.

respectively. The hexadecane contact angle on the virgin membrane was found to be significantly higher (99 ± 3°), explained by the long alkyl chain of the oil: the numerous -CH_2 functional groups are more likely to interact with a polymer of a similar nature, that is containing numerous methylene groups. It is for instance expected that polypropylene would be better wetted by hexadecane than PVDF. It is also interesting to note the effect of the membrane structure on its wetting properties: in a previous work, we reported lower oil contact angles under water of virgin PVDF membranes prepared by VIPS. The virgin membrane, however and unlike the present virgin membrane, possessed a different structure as it was prepared from a casting solution containing 25 wt% polymer and dissolved at 50 °C, resulting in much larger nodules. Consequently, it was both more hydrophobic and more oleophilic [57]. Secondly, the oil contact angle was drastically increased for both ST0SB100 and ST40SB60 membranes. This increase of surface oleophobicity confirmed one more time the deposition of SBMA. Thirdly, the OCA was in the same range for both ST0SB100 and ST40SB60 membranes, regardless of the nature of the oil. For example, the toluene contact angle was found to be 145 ± 3° and 148 ± 3° on ST0SB100 and ST40SB60 membranes, respectively. This observation indicates that SBMA dominates the wetting behavior of the membranes by the oil: there is no need for 100% SBMA to reach oleophobicity. This is supported by the OCA results obtained with ST100SB0: 100% styrene is necessary to maintain significant wetting of the membrane by the oil. Fourthly, the OCA of the ST100SB0 membrane is strongly dependent on the nature of the oil. It appears that hexane and hexadecane do not spread onto ST100SB0, revealing very little affinity between the phenyl groups of polystyrene and the pure hydrogenated oils. On the contrary, toluene, a mono-substitute benzene derivative, wets ST100SB0 given the chemical structure similarities with styrene. Importantly, ST40SB60 membrane is oleophobic under water and as it is also hydrophilic, it is potentially suitable for the breaking of O/W emulsions.

3.3. Separation of oil-in-water emulsions

The ST40SB60 membrane which was identified in Section 3.1 as the membrane fitting best our needs for O/W separation was tested in the separation of various O/W emulsions. Toluene, hexane, hexadecane, diesel and soybean oil were mixed with water in order to form stable emulsions (at least stable over the duration of the membrane separation process). The total permeate weight was recorded over time and corresponding transient fluxes plotted (Fig. 7a and b) until a plateau was reached indicating the end of the tests. In addition, the separation efficiency was determined from the measurements of the water content in the permeate and the knowledge of the initial feed compositions (Fig. 7c). Photographs and microscopy images are also provided to visually assess the quality of the separation (Fig. 7d and S7). Before starting to describe and discuss the results, it is important to stress that no permeation was obtained with the virgin membrane in the filtration conditions used. Moreover, physical parameters that can drastically influence the separation of O/W emulsions such as the surface roughness or membrane pore size will not be discussed here as only ST40SB60 membrane was used.

Fig. 7 shows that the transient flux is affected by the nature of the oil forming the emulsion. In particular, it is seen that the separation tends to be faster when lower molecular weight-oils are at play (toluene or hexane) while it is much lengthier for larger molecular weight-oils and mixture of oils (diesel, soybean oil). The difference cannot be explained by different wetting behaviors by the dispersing phase as it is water in all cases, while similar wetting by the dispersed phase were obtained regardless of the nature of the oil (Fig. 6). However, different emulsion sizes may play a key role and influence the different permeation fluxes observed. Fig. 8 highlights important differences in the emulsion size with the nature of the oil, for similar preparation conditions: the smallest emulsions are obtained with hexadecane, soybean and diesel oils while the largest ones are obtained with lower molecular weight oils (toluene and hexane). As the emulsion size increases and for similar oil contents, it is reasonable to assume that the total number of oil droplets dispersed in water decreases. As a consequence, fewer of these droplets needs to be broken to unable the separation, hence the faster

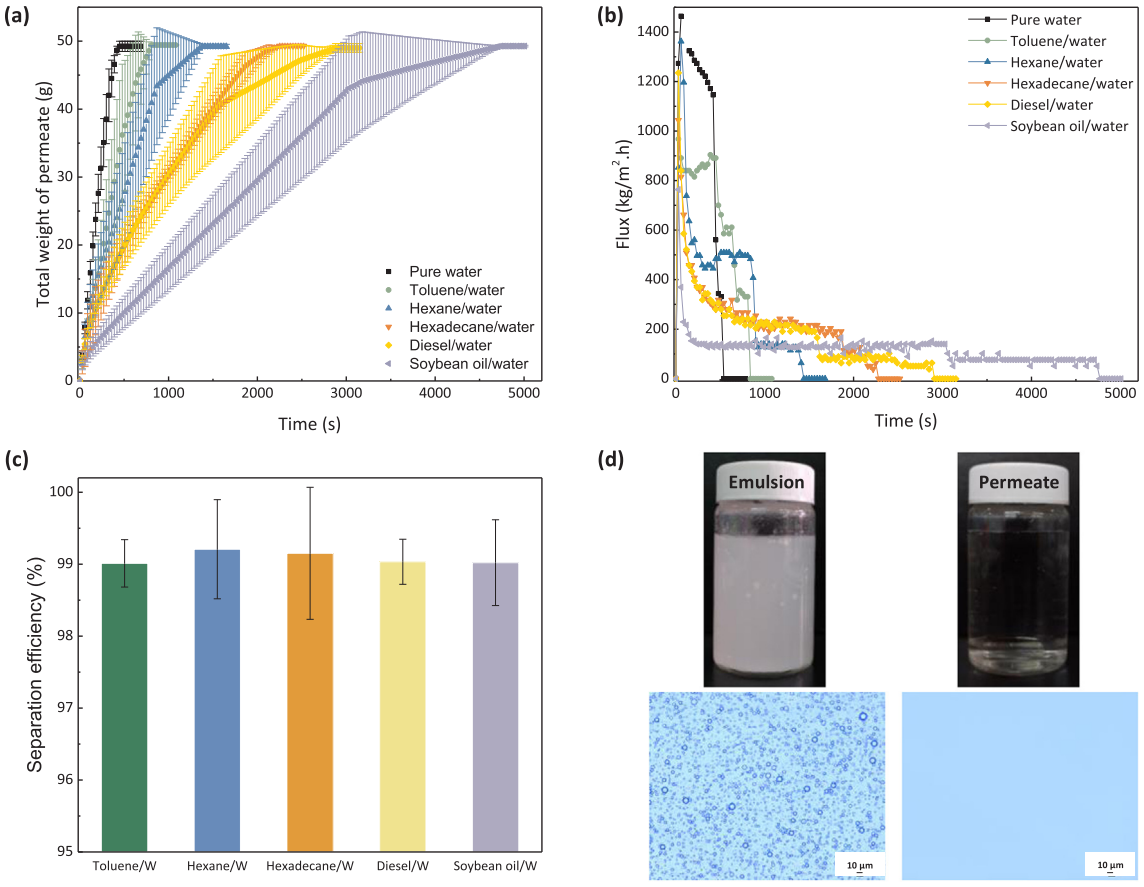

Fig. 7. Membrane separation of O/W emulsions. (a) Permeate weight as a function of time; (b) Average flux obtained from (a); (c) Separation efficiency; (d) Photos and microscopy images of the initial soybean oil/W emulsion and of the permeate after filtration.

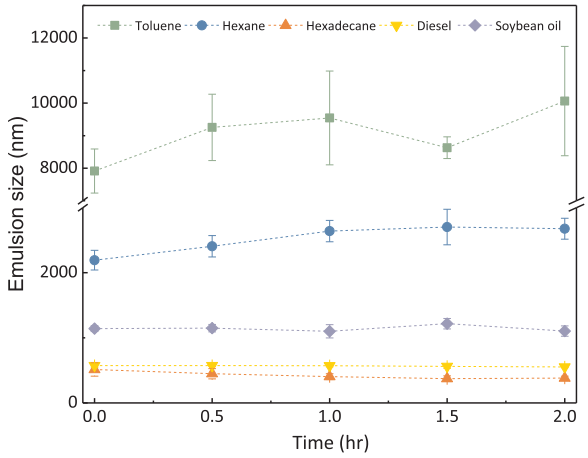

Fig. 8. Size of the different O/W emulsions and their stability over time.

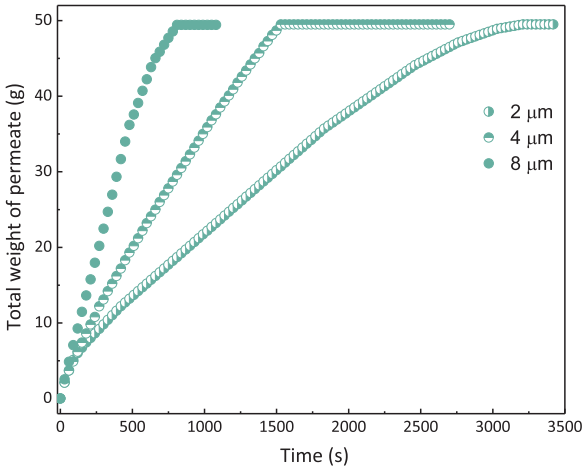

Fig. 9. The effect of the toluene/water emulsion size on the permeation rates of the ST40SB60 membrane.

permeation rates recorded. To check this assumption, toluene/W emulsions were prepared by changing the parameters of the sonication bath or by using a sonication probe, in order to obtain emulsions which size would be approximately 2 µm, 4 µm and 8 µm. Then, filtration tests were performed and the related results are graphed in Fig. 9. The plot of the permeate weight vs. time corresponding to the 8 µm-emulsion is similar to that reported in Fig. 7a. However, the results clearly indicate that the emulsion size importantly affects the separation rates of the membranes, which explains why it took longer to separate soybean/W, hexadecane/W and diesel/W emulsions during the tests which results were presented in Fig. 7.

The separation efficiency was determined, using the Karl-Fisher method that enables to determine the water content in each phase. The related results are presented in Fig. 7d. The separation efficiencies obtained were very high, each time higher than 99%, which shows the versatility of the membrane. More precisely, they were measured to be 99.0 ± 0.3%, 99.2 ± 0.7%, 99.2 ± 0.9%, 99.0% ± 0.3% and 99.0% ± 0.6%, for toluene/W, hexane/W, hexadecane/W, diesel/W and soybean oil/W, respectively. These high separation efficiencies are very similar to those very recently reported in literature using other systems [27,28,31], which also highlights the suitability of the short cut (synthesis and self-assembling) used to hydrophilize the membranes. It

is also seen that the separation is as efficient for low molecular weight oils as it is for larger molecular weight oils and mixture of oils. Indeed, the separation of efficiency of hexadecane/W is as good as that obtained with hexane/W, which clearly shows that there is no impact of the alkane chain length on the separation efficiency. Although it is not seen from the contact angle measurements, which only involve one droplet of pure oil contacted with the membrane for a short time, longer alkanes will have a higher tendency to swell (and in the worst case, to damage) the polymer membrane, which could affect the separation efficiency. Yet, no separation efficiency differences were measured, hence proving the suitability of surface-modified PVDF VIPS membranes to separate O/W emulsions containing oils made of either long or short alkyl chains. Soybean oil [58] and diesel [59] are mixtures of high molecular weight oils, which enhances the complexity of the separation as each oil component wets and swells the membrane in a different extent. Yet, despite the fact that lower separation rates were obtained with these oils, the separation efficiency (99.0%) remained high, which indicates that the as-prepared membranes are actual potential efficient materials for the treatment of O/W emulsions from either the petroleum or the vegetable oil industry.

4. Conclusions

This study has presented the surface hydrophilization of PVDF membranes prepared by VIPS, by a process during which the zwitterionic polymer, PS-*r*-PSBMA, is both synthesized and self-assembled onto the membranes in one single step. This process enables to address the solubility issues of zwitterionic polymers, as there is no need to find a solvent for the zwitterionic polymer, as it would be required in common coating or in-situ modification processes. After an optimization of the surface-modification procedures, the membranes were then fully characterized and used in the separation of various O/W emulsions. The essential results are as follows:

- A styrene/SBMA molar ratio: 40/60; a total solid content of 5 wt% and a reaction time of 5 h led to the most hydrophilic membrane, presenting a WCA of 12°;
- A surface chemistry analysis revealed that the actual styrene/SBMA molar ratios at the surface of the membrane were closed to the initial molar ratios in the reactive solutions, but homogeneous membranes were only obtained for ratios close to 1;
- The optimized membrane, named ST40SB60, was found to be superhydrophilic and highly oleophobic under water, using 5 different oils including toluene, hexane, hexadecane, diesel and soybean oil.
- 5 different O/W emulsions were prepared and separated by membrane filtration under low transmembrane pressure (0.5 atm). Whether model oils were used (toluene, hexane, hexadecane) or commercial oils (diesel, soybean oil), a very high separation efficiency (> 99%) was obtained in each case, leading to an almost oil-free permeate.
- The separation rates obtained depended on the size of the emulsion at play. For similar preparation conditions, toluene/W and hexane/W droplets were larger, hence leading to much faster separation than hexadecane/W, diesel/W and soybean oil/W.

Overall, this study showed the suitability of hydrophilized PVDF VIPS membrane for oily wastewater treatment, provided an adequate surface modification, although efforts are still needed to enhance separation rates, and to evaluate the extent of membrane fouling by oil during filtration of larger volumes, or during continuous filtration tests.

Acknowledgments

The first author expresses his sincere gratitude to the Ministry of Science and Technology of Taiwan (MOST) for founding this work through the Outstanding young researcher research grant (MOST 106–2628-E-033 – 002 -MY3). In addition, complementary funding was brought in the frame of the SuperHYM project co-funded by MOST and the French National Research Agency (MOST 106–2923-E-033-001-MY4 and ANR-16-CE08–0037-01).

Appendix A. Supplementary material

Supplementary data associated with this article can be found in the online version at http://dx.doi.org/10.1016/j.memsci.2018.05.049.

References

[1] A.B. Nordvik, J.L. Simmons, K.R. Bitting, A. Kewis, T. Strøm-Kristiansen, Oil and water separation in marine oil spill clean-up operations, Spill Sci. Technol. Bull. 3 (1996) 107–122.
[2] A.A. Al-Shamrani, A. James, H. Xiao, Destabilisation of oil–water emulsions and separation by dissolved air flotation, Water Res. 36 (2002) 1503–1512.
[3] A. Cambiellam, J.M. Benito, C. Pazos, J. Coca, Centrifugal separation efficiency in the treatment of waste emulsified oils, Chem. Eng. Res. Des. 84 (2006) 69–76.
[4] N.M. Kocherginsky, C.L. Tan, W.F. Lu, Demulsification of water-in-oil emulsions via filtration through a hydrophilic polymer membrane, J. Membr. Sci. 220 (2003) 117–128.
[5] H.J. Li, Y.M. Cao, J.J. Qin, X.M. Jie, T.H. Wang, J.H. Liu, Q. Yuan, Development and characterization of anti-fouling cellulose hollow fiber UF membranes for oil-water separation, J. Membr. Sci. 279 (2006) 328–335.
[6] W. Chen, J. Peng, Y. Su, L. Zheng, L. Wang, Z. Jiang, Separation of oil/water emulsion using Pluronic F127 modified polyethersulfone ultrafiltration membranes, Sep. Purif. Technol. 66 (2009) 591–597.
[7] A. Ezzati, E. Gorouhi, T. Mohammadi, Separation of water in oil emulsions using microfiltration, Desalination 185 (2005) 371–382.
[8] P. Bernardo, E. Drioli, Membrane technology: latest applications in the refinery and petrochemical field, Compr. Membr. Sci. Eng. 4 (2010) 211–239.
[9] X. Zhu, H.E. Loo, R. Bai, A novel membrane showing both hydrophilic and oleophobic surface properties and its non-fouling performances for potential water treatment applications, J. Membr. Sci. 436 (2013) 47–56.
[10] F.E. Ahmed, B.S. Lalia, N. Hilal, R. Hashaikeh, Underwater superoleophobic cellulose/electrospun PVDF–HFP membranes for efficient oil/water separation, Desalination 344 (2014) 48–54.
[11] R. Zolfaghari, A. Fakhru'l-Razi, L.C. Abdullah, S.S.E.H. Elnashaie, A. Pendashteh, Demulsification techniques of water-in-oil and oil-in-water emulsions in petroleum industry, Sep. Purif. Technol. 170 (2016) 377–407.
[12] Z. Šereš, N. Maravić, A. Takači, I. Nikolić, D. Šoronja-Simović, A. Jokić, C. Hodur, Treatment of vegetable oil refinery wastewater using alumina ceramic membrane: optimization using response surface methodology, J. Clean. Prod. 112 (2016) 3132–3137.
[13] D.W. Zhao, I.D. Gates, On hot water flooding strategies for thin heavy oil reservoirs, Fuel 153 (2015) 559–568.
[14] M.J. Barnaji, P. Pourafshary, M.R. Rasaie, Visual investigation of the effects of clay minerals on enhancement of oil recovery by low salinity water flooding, Fuel 184 (2016) 826–835.
[15] A.E. Atabani, A.S. Silitonga, H.C. Ong, T.M.I. Mahlia, H.H. Masjuki, Irfan Anjum Badruddin, H. Fayaz, Non-edible vegetable oils: a critical evaluation of oil extraction, fatty acid compositions, biodiesel production, characteristics, engine performance and emissions production, Renew. Sustain. Energy Rev. 18 (2013) 211–245.
[16] M.V. Tres, S. Mohr, M.L. Corazza, M. Di Luccio, J.V. Oliveira, Separation of n-butane from soybean oil mixtures using membrane processes, J. Membr. Sci. 33 (2009) 141–146.
[17] S. Manjula, H. Nabetani, R. Subramanian, Flux behavior in a hydrophobic dense membrane with undiluted and hexane-diluted vegetable oils, J. Membr. Sci. 366 (2011) 43–47.
[18] E. Ankyu, R. Noguchi, Economical evaluation of introducing oil-water separation technology to wastewater treatment of food processing factory based on separation engineering, Agric. Agric. Sci. Procedia 2 (2014) 67–73.
[19] J. Yong, Y. Fang, F. Chen, J. Huo, Q. Yang, H. Bian, G. Du, X. Hou, Femtosecond laser ablated durable superhydrophobic PTFE films with micro-through-holes for oil/water separation: separating oil from water and corrosive solutions, Appl. Surf. Sci. 389 (2016) 1148–1155.
[20] J.-J. Li, L.-T. Zhu, Z.-H. Luo, Electrospun fibrous membrane with enhanced switchable oil/water wettability for oily water separation, Chem. Eng. J. 287 (2016) 474–481.
[21] J. Liu, P. Li, L. Chen, Y. Feng, W. He, X. Lv, Modified superhydrophilic and underwater superoleophobic PVDF membrane with ultralow oil-adhesion for highly efficient oil/water emulsion separation, Mater. Lett. 185 (2016) 169–172.
[22] J. Liu, P. Li, L. Chen, Y. Feng, W. He, X. Yan, X. Lü, Superhydrophilic and underwater superoleophobic modified chitosan-coated mesh for oil/water separation, Surf. Coat. Technol. 307 (2016) 171–176.
[23] J.A. Prince, S. Bhuvana, V. Anbharasi, N. Ayyanar, K.V.K. Boodhoo, G. Singh, Ultra-wetting graphene-based PES ultrafiltration membrane - A novel approach for successful oil-water separation, Water Res. 103 (2016) 311–318.
[24] H. Shi, Y. He, Y. Pan, H. Di, G. Zheng, L. Zhang, C. Zhang, A modified mussel-inspired method to fabricate TiO_2 decorated superhydrophilic PVDF membrane for

oil/water separation, J. Membr. Sci. 506 (2016) 60–70.
[25] L. Chen, Y. Si, H. Zhu, T. Jiang, Z. Guo, A study on the fabrication of porous PVDF membranes by in-situ elimination and their applications in separating oil/water mixtures and nano-emulsions, J. Membr. Sci. 520 (2016) 760–768.
[26] F. Zhang, S. Gao, Y. Zhu, J. Jin, Alkaline-induced superhydrophilic/underwater superoleophobic polyacrylonitrile membranes with ultralow oil-adhesion for high efficient oil/water separation, J. Membr. Sci. 513 (2016) 67–73.
[27] Q. Yang, A. Gao, L. Xue, "Butterfly Effect" from finite dope chemical composition variations on the water/oil separation capabilities of super rough polyvinylidene difluoride (PVDF) porous membranes, J. Membr. Sci. 524 (2017) 197–204.
[28] B. Cheng, Z. Li, Q. Li, J. Ju, W. Kang, M. Naebe, Development of smart poly(vinylidene fluoride)-graft-poly(acrylic acid) tree-like nanofiber membrane for pH-responsive oil/water separation, J. Membr. Sci. 534 (2017) 1–8.
[29] W. Qing, X. Shi, Y. Deng, W. Zhang, J. Wang, C.Y. Tang, Robust superhydrophobic-superoleophilic polytetrafluoroethylene nanofibrous membrane for oil/water separation, J. Membr. Sci. 540 (2017) 354–361.
[30] Y. Liu, Y. Su, J. Cao, J. Guan, R. Zhang, M. he, L. Fan, Q. Zhang, Z. Jiang, Antifouling, high-flux oil/water separation carbon nanotube membranes by polymer-mediated surface charging and hydrophilization, J. Membr. Sci 542 (2017), pp. 254–263.
[31] Y. Liao, M. Tian, R. Wang, A high-performance and robust membrane with switchable superwettability for oil/water separation under ultralow pressure, J. Membr. Sci. 543 (2017) 123–132.
[32] Y. Jiang, J. Hou, J. Xu, B. Shan, Switchable oil/water separation with efficient and robust Janus nanofiber membranes, Carbon 115 (2017) 477–485.
[33] X. Yang, Y. He, G. Zeng, X. Chen, H. Shi, D. Qing, F. Li, Q. Chen, Bio-inspired method for preparation of multiwall carbon nanotubes decorated superhydrophilic poly(vinylidene fluoride) membrane for oil/water emulsion separation, Chem. Eng. J. 321 (2017) 245–256.
[34] P.-Y. Chen, S.-H. Tung, One-step electrospinning to produce nonsolvent-induced macroporous fibers with ultrahigh oil adsorption capability, Macromolecules 50 (2017) 2528–2534.
[35] J. Li, C. Xu, H. Tian, F. Zha, W. Qi, Q. Wang, Blend-electrospun poly(vinylidene fluoride)/stearic acid membranes for efficient separation of water-in-oil emulsions, Colloids Surf., A 538 (2018) 494–499.
[36] J. Cao, Z. Cheng, L. Kang, M. Chu, D. Wu, M. Li, S. Xie, R. Wen, Novel stellate poly (vinylidene fluoride)/polyethersulfone microsphere-nanofiber electrospun membrane with special wettability for oil/water separation, Mater. Lett. 207 (2017) 190–194.
[37] M. Obaid, H.O. Mohamed, A.S. Yasin, M.A. Yassin, O.A. Fadali, H. Kim, N.A.M. Barakat, Water Res. 123 (2017) 524–535.
[38] J. Zhao, Q. Shi, S. Luan, L. Song, H. Yang, H. Shi, J. Jin, X. Li, J. Yin, P. Stagnaro, Improved biocompatibility and antifouling property of polypropylene non-woven fabric membrane by surface grafting zwitterionic polymer, J. Membr. Sci. 369 (2011) 5–12.
[39] M.-Z. Li, J.-H. Li, X.-S. Shao, J. Miao, J.-B. Wang, Q.-Q. Zhang, X.-P. Xu, Grafting zwitterionic brush on the surface of PVDF membrane using physisorbed free radical grafting technique, J. Membr. Sci. 405- 406 (2012) 141–148.
[40] J.-F. Jhong, A. Venault, C.H. Hou, S.-H. Chen, T.-C. Wei, J. Zheng, J. Huang, Y. Chang, Surface zwitterionization of expanded poly(tetrafluoroethylene) membranes via atmospheric plasma-induced polymerization for enhanced skin wound healing, ACS Appl. Mater. Interfaces 5 (2013) (6762-6742).
[41] T. Xiang, T. Lu, Y. Xie, W.-F. Zhao, S.-D. Sun, C.-S. Zhao, Zwitterionic polymer functionalization of polysulfone membrane with improved antifouling property and blood compatibility by combination of ATRP and click chemistry, Acta Biomater. 40 (2016) 162–171.
[42] R. Zhou, P.-F. Ren, H.-C. Yang, Z.-K. Xu, Fabrication of antifouling membrane surface by poly(sulfobetaine methacrylate)/polydopamine co-deposition, J. Membr. Sci. 466 (2014) 18–25.
[43] D.J. Lin, K. Beltsios, T.H. Young, Y.S. Jeng, L.P. Cheng, Strong effect of precursor preparation on the morphology of semicrystalline phase inversion poly(vinylidene fluoride) membranes, J. Membr. Sci. 274 (2006) 64–72.
[44] C.L. Li, D.M. Wang, A. Deratani, D. Quemener, D. Bouyer, J.Y. Lai, Insight into the preparation of poly(vinylidene fluoride) membranes by vapor-induced phase separation, J. Membr. Sci. 361 (2010) 154–166.
[45] A. Venault, Y. Chang, D.-M. Wang, D. Bouyer, A. Higuchi, J.-Y. Lai, PEGylation of anti-biofouling polysulfone membranes via liquid- and vapor-induced phase separation processing, J. Membr. Sci. 403- 404 (2012) 47–57.
[46] S.T. Kao, M.Y. Teng, C.L. Li, C.Y. Kuo, C.Y. Hsieh, H.A. Tsai, D.M. Wang, K.R. Lee, J.Y. Lai, Fabricating PC/PAN composite membranes by vapor-induced phase separation, Desalination 233 (2008) 96–103.
[47] M. Gu, J. Zhang, X. Wang, H. Tao, L. Ge, Formation of poly(vinylidene fluoride) (PVDF) membranes via thermally induced phase separation, Desalination 192 (2006) 160–167.
[48] W. Zhang, Y. Zhu, X. Liu, D. Wang, J. Li, L. Jiang, J. Jin, Salt-induced fabrication of superhydrophilic and underwater superoleophobic PAA-g-PVDF membranes for effective separation of oil-in-water emulsions, Angew. Chem. 126 (2014) 875–879.
[49] Y.-C. Chiag, Y. Chang, W.-Y. Chen, R.-C. Ruaan, Biofouling resistance of ultrafiltration membranes controlled by surface self-assembled coating with PEGylated copolymers, Langmuir 28 (2012) 1399–1407.
[50] N.J. Lin, H.S. Yang, Y. Chang, K.L. Tung, W.H. Chen, H.W. Cheng, S.W. Hsiao, P. Aimar, K. Yamamoto, J.Y. Lai, Surface self-assembled PEGylation of fluoro based PVDF membranes via hydrophobic-driven copolymer anchoring for ultra-stable biofouling resistance, Langmuir 29 (2013) 10183–10193.
[51] D. Freitas Siqueira, F. Galembeck, S. Pereira Nunes, Adhesion and morphology of PVDF/PMMA and compatibilized PVDF/PS interfaces, Polymer 32 (1991) 990–998.
[52] Y.-N. Chou, Y. Chang, T.-C. Wen, Applying thermosettable zwitterionic copolymers as general fouling-resistant and thermal-tolerant biomaterial interfaces, ACS Appl. Mater. Interfaces 7 (2015) 10096–10107.
[53] P.-F. Ren, Y. Fang, L.-S. Wan, X.-Y. Ye, Z.-K. Xu, Surface modification of polypropylene microfiltration membrane by grafting poly(sulfobetaine methacrylate) and poly(ethylene glycol): oxidative stability and antifouling capability, J. Membr. Sci. 492 (2015) 249–256.
[54] D. Saviello, E. Pouyet, L. Toniolo, M. Cotte, A. Nevin, Synchrotron-based FTIR microspectroscopy for the mapping of photo-oxidation and additives in acrylonitrile–butadiene–styrene model samples and historical objects, Anal. Chim. Acta 843 (2014) 59–72.
[55] M. You, P. Wang, M. Xu, T. Yuan, J. Meng, Fouling resistance and cleaning efficiency of stimuli-responsive reverse osmosis (RO) membranes, Polymer 103 (2016) 457–467.
[56] O.M. Ba, P. Marmey, K. Anselme, A.C. Duncan, A. Ponche, Surface composition XPS analysis of a plasma treated polystyrene: evolution over long storage periods, Colloid Surf., B 145 (2016) 1–7.
[57] A. Venault, A.J. Jumao-as-Leyba, F.-C. Chou, D. Bouyer, I.-J. Lin, T.-C. Wei, Y. Chang, Design of near-superhydrophobic/superoleophilic PVDF and PP membranes for the gravity-driven breaking of water-in-oil emulsions, J. Taiwan Inst. Chem. Eng. 65 (2016) 459–471.
[58] B. Gao, Y. Luo, W. Lu, J. Liu, Y. Zhang, L. Yu, Triacylglycerol compositions of sunflower, corn and soybean oils examined with supercritical CO_2 ultra-performance convergence chromatography combined with quadrupole time-of-flight mass spectrometry, Food Chem. 218 (2017) 569–574.
[59] W. Kiatkittipong, S. Phimsen, K. Kiatkittipong, S. Wongsakulphasatch, N. Laosiripojana, S. Assabumrungrat, Diesel-like hydrocarbon production from hydroprocessing of relevant refining palm oil, Fuel Process. Technol. 116 (2013) 16–26.